ADVANCES IN ATMOSPHERIC SCIENCES, VOL. 35, JUNE 2018, 682–688

• **Original Paper** •

Impact of the Spring SST Gradient between the Tropical Indian Ocean and Western Pacific on Landfalling Tropical Cyclone Frequency in China

Lei WANG* and Guanghua CHEN

Center for Monsoon System Research, Institute of Atmospheric Physics, Chinese Academy of Sciences, Beijing 100029*, China*

(Received 5 April 2017; revised 7 September 2017; accepted 21 November 2017)

ABSTRACT

The present study identifies a significant influence of the sea surface temperature gradient (SSTG) between the tropical Indian Ocean (TIO; 15°S–15°N, 40°–90°E) and the western Pacific warm pool (WWP; 0°–15°N, 125°–155°E) in boreal spring on tropical cyclone (TC) landfall frequency in mainland China in boreal summer. During the period 1979–2015, a positive spring SSTG induces a zonal inter-basin circulation anomaly with lower-level convergence, mid-tropospheric ascendance and upper-level divergence over the west-central TIO, and the opposite situation over the WWP, which produces lower-level anomalous easterlies and upper-level anomalous westerlies between the TIO and WWP. This zonal circulation anomaly further warms the west-central TIO by driving warm water westward and cools the WWP by inducing local upwelling, which facilitates the persistence of the anomaly until the summer. Consequently, lower-level negative vorticity, strong vertical wind shear and lower-level anticyclonic anomalies prevail over most of the western North Pacific (WNP), which decreases the TC genesis frequency. Meanwhile, there is an anomalous mid-tropospheric anticyclone over the main WNP TC genesis region, meaning a westerly anomaly dominates over coastal regions of mainland China, which is unfavorable for steering TCs to make landfall in mainland China during summer. This implies that the spring SSTG may act as a potential indicator for TC landfall frequency in mainland China.

Key words: tropical cyclone, landfall, sea surface temperature gradient, air–sea interaction

Citation: Wang, L., and G. H. Chen, 2018: Impact of the spring SST gradient between the tropical Indian Ocean and western Pacific on landfalling tropical cyclone frequency in China. *Adv. Atmos. Sci.*, **35**(6), 682–688, https://doi.org/10.1007/s00376-017-7078-2.

1. Introduction

Tropical cyclone (TC) landfall activity is very frequent over the west coasts of the western North Pacific (WNP), especially in mainland China. During the period 1979–2015, the annual mean number of landfalling TCs (LTCs) in mainland China was greater than seven, among which five occurred in summer on average. In this peak season, LTCs cause serious disasters in Chinese coastal regions. Seasonal forecasting factors modulating TC landfall frequency in South China, such as El Niño–Southern Oscillation (ENSO), have been investigated (e.g., Liu and Chan, 2003; Goh and Chan, 2010). Moreover, previous studies have pointed out that TC landfall activity is closely related to TC genesis location and steering flow (Liu and Chan, 2003; Wu et al., 2004; Goh and Chan, 2010; Mei et al., 2015). Generally, TC genesis depends largely on favorable environmental fields, such as low-level relative vorticity, vertical wind shear, and sea surface temperature (SST) (Gray, 1979; Emanuel, 2003; Li and Zhou, 2012). The TC steering flow can be measured by large-scale mid-tropospheric flow (Chan and Gray, 1982) and is largely responsible for TC tracks (Ho et al., 2004). In seasonal TC forecasts, TC landfall in a targeted area is of more concern, but numerous errors still sometimes appear due to our limited understating (Zhan et al., 2012). Therefore, it is imperative to explore reliable factors and shed light on the key mechanisms involved in the interannual variation of LTCs in mainland China.

The dynamic and thermodynamic conditions mentioned above can be significantly modulated by atmospheric teleconnection and air–sea interaction associated with SST gradients (SSTGs) during the TC season. In the Atlantic, the seasonal hurricane activity can be directly impacted by the SSTG between the North and South Atlantic (Kossin and Vimont, 2007; Vimont and Kossin, 2007). In the Pacific, the spring SSTG between the southwestern Pacific and the western Pacific warm pool (WWP) has been identified as a new factor controlling TC genesis frequency in the typhoon season (June–October) (Zhan et al., 2013). A follow-up study (Zhao et al., 2016) indicated that the connection between them intensified after the mid-1970s, as compared to the period 1951–74. The SSTG anomaly in the Atlantic can persist through the hurricane season and directly modulate hur-

* Corresponding author: Lei WANG
Email: wl@mail.iap.ac.cn

ricane activity, whereas the Pacific SSTG weakens rapidly after spring and influences TC genesis via the persistence of the preconditioned atmospheric circulation based on the air–sea interaction. In these individual basins, both the Atlantic and Pacific SSTG anomalies show a meridional distribution.

Recently, the zonal response of atmospheric circulation over the WNP to Indian Ocean (IO) SST change has become an area of interest. In summer, northwestern IO cooling leads to an anomalous cyclone over the subtropical WNP (Wang and Wu, 2012). Via a baroclinic Kelvin wave, tropical IO (TIO) warming can induce an anomalous anticyclone and suppressed convection over the WNP throughout summer after El Niño, followed by dissipation in spring (Yang et al., 2007; Xie et al., 2009), which decreases the summer TC frequency over the WNP (Du et al., 2011). Besides, the effect of eastern IO SST anomalies on TC genesis over the WNP has been confirmed in numerical experiments with specified SST forcing in the eastern IO (Zhan et al., 2011b). The eastern IO SST in spring can be regarded as a seasonal predictor for WNP TC activity (Zhan et al., 2011a). Compared with ENSO, the TIO SST has a more direct and significant effect on WNP TC activity during El Niño and La Niña decaying years (Tao et al., 2012). Through air–sea interaction, the summertime TC genesis over the South China Sea can be modulated by the zonal SSTG between the northern IO and the WNP (Li and Zhou, 2014). Furthermore, inter-basin air–sea interaction can create positive feedback between the northern IO warming and the anomalous anticyclone spanning the tropical WNP and the northern IO (Xie et al., 2016).

Few studies on the relationship between LTC activity and SSTGs, especially zonal SSTGs, have been conducted. In view of the significant seasonal relationship between WNP TC activity and the zonal inter-basin atmospheric circulation induced by SST, we focus on the possible influence of the spring SSTG between the TIO and WWP on the LTC frequency in mainland China in summer. We begin by identifying the LTCs in mainland China and the regions of the zonal SSTG. The relationship between the LTC frequency and the SSTG is then explained by investigating the air–sea interaction that impacts the genesis frequency and location of WNP TCs and the large-scale steering flows.

2. Data and methodology

Monthly mean ERA-Interim data from the European Centre for Medium-Range Weather Forecasts (Dee et al., 2011) and SST data from the Met Office Hadley Centre (Rayner et al., 2003) are used to identify the relationship between the SSTG and large-scale circulation anomalies over the WNP from 1979 to 2015. In the same period, the TC best-track data (including LTC position and time) from the International Best Tracks Archive for Climate Stewardship (IBTrACS) project (Knapp et al., 2010) are used to investigate the LTC information. A current time record is regarded as a TC landfall record if the minimum distance from a TC to land between the current time and the next reporting time is zero in the IBTrACS data. These data undergo quality control and combine information from numerous TC datasets, such as the Joint Typhoon Warning Center, China Meteorological Administration, and Hong Kong Observatory.

The IBTrACS data provide an LTC record without isolating the LTCs in mainland China. As shown in Fig. 1, if any of the TC landfall location lies within the region enclosed by the blue line, it is regarded as an LTC in mainland China and its first landfall record in the region can be identified as the landfall location and time. According to this criterion, 185 TCs made landfall in mainland China in summer during the period 1979–2015. Manual examination verifies that LTCs in mainland China can be identified effectively using this key region. The LTC frequency is defined as the annual number of LTCs in mainland China in summer. In addition, correlation analysis is used to reveal the relationship between the SSTG and LTC frequency in mainland China. Regression and composite analyses are applied to investigate the response of the atmospheric circulation to the SSTG.

3. Relationship between the SSTG and LTC frequency

To investigate whether the spring zonal SSTG plays a role in the interannual variation of summertime LTC frequency in mainland China, the correlation coefficients between the LTC frequency in mainland China and the SST are shown in Fig. 2. There are significant negative correlations in the TIO and positive correlations in the WWP. In this study, the zonal SSTG is defined as the difference between the SST averaged over the TIO (15°S–15°N, 40°–90°E) and that averaged over the WWP (0°–15°N, 125°–155°E). A positive (negative) SSTG is thus related to warmer (cooler) SST over the TIO and cooler (warmer) SST in the WWP.

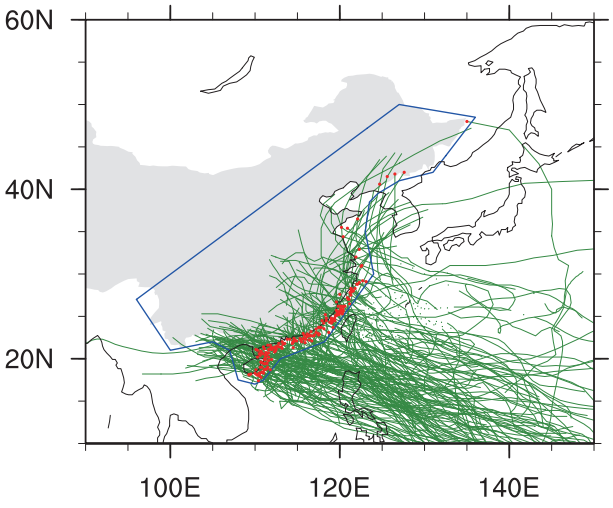

Fig. 1. Tracks (green lines) and landfall locations (red dots indicate LTC center positions) of LTCs in mainland China identified by the region enclosed within the blue line in summer (June–August) during 1979–2015. Green dots denote disconnected LTC tracks due to missing values in the IBTrACS data.

Moreover, we compare the variations of the zonal inter-basin SSTG and the LTC frequency in mainland China. Figure 3a shows the lag correlations between the monthly SSTG and the LTC frequency in mainland China during boreal summer (June–August). The correlation coefficients display significance at the 99% confidence level from February to June. In March, the correlation coefficients are at their highest, reaching about −0.50. Given the significant relationship

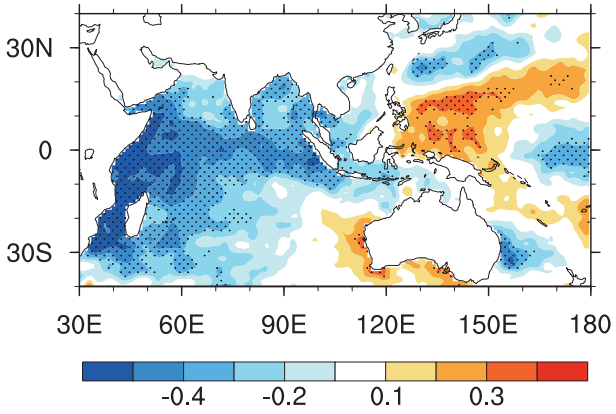

Fig. 2. Distribution of correlation coefficients between spring (March–May) SST and summer (June–August) LTC frequency in mainland China during 1979–2015. Stippling denotes regions where correlation coefficients are significant at the 90% confidence level.

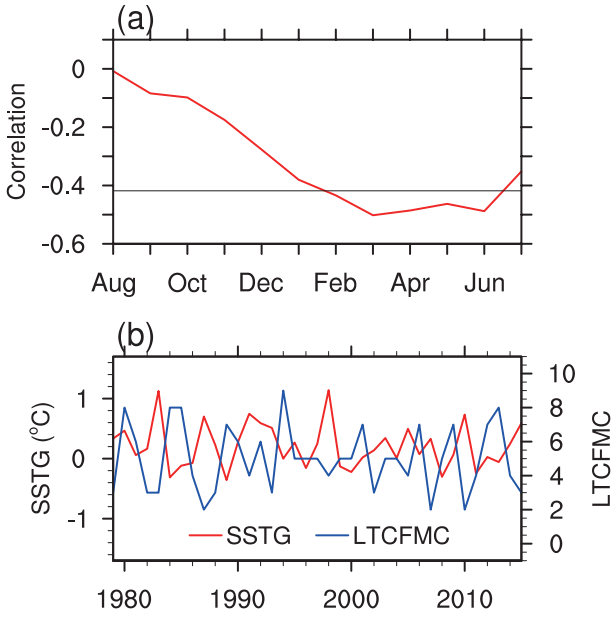

Fig. 3. (a) Correlation between LTC frequency in mainland China (LTCFMC) in summer (June–August) and the monthly SSTG between the TIO (15°S–15°N, 40°–90°E) and the WWP (0°–15°N, 125°–155°E) from the preceding August to July during 1979–2015. (b) Time series of LTCs in summer and the SSTG in spring (March–May) for 1979–2015. The solid transverse line in (a) indicates correlations significant at the 99% confidence level.

Table 1. Annual SST in spring, annual LTC frequency in mainland China (LTCFMC), and the steering flow anomaly over Chinese coastal regions (SFACCR) in summer, related to positive and negative SSTGs during 1979–2015.

	Annual SST in spring (°C)		Annual LTCFMC in summer	SFACCR in summer
	TIO	WWP		
Positive SSTG	29.18	28.80	4.50	westerly
Negative SSTG	28.87	29.05	6.18	easterly

appearing in spring (March–May), this paper focuses on the influence of the spring SSTG on summer LTCs. Their time series are shown in Fig. 3b, revealing a close relationship with correlation coefficients of about −0.51, exceeding the 99% significance level. Table 1 shows that the annual mean LTC frequency during the 11 negative SSTG years is 1.6 more than that during the 26 positive SSTG years.

4. Possible physical mechanism

Figure 4 shows the regressed seasonal mean 850-hPa and 200-hPa divergent winds and velocity potential, sea level pressure (SLP), and 500-hPa vertical pressure velocity in summer with respect to the spring SSTG. A positive SSTG reduces (enhances) the SLP over the TIO (WWP), which causes distinct inter-basin circulation anomalies. There is an obvious convergence over the TIO and divergence over the WWP at the lower level. Meanwhile, divergence over the Arabian Sea and convergence over the WWP are also evident, at the upper level. Corresponding to these circulation anomalies, mid-tropospheric ascent over the TIO and descent over the tropical western Pacific are apparent. Between the TIO and WWP, lower-level anomalous easterlies and upper-level anomalous westerlies are produced. This zonal circulation anomaly accords with the atmospheric responses to the positive SSTG.

Moreover, the zonal circulation anomaly mentioned above also hints at anomalous SST warming (cooling) in the TIO (WWP). Triggered by the positive springtime SSTG, the lower-level anomalous convergent winds over the TIO in Fig. 4a act to warm the western-central TIO by inhibiting oceanic upwelling and driving warm water toward this basin due to the anomalous lower-level easterlies from the western Pacific. Meanwhile, the lower-level anomalous divergent winds in Fig. 4a act to cool the WWP by inducing local upwelling. It is via this air–sea interaction that the zonal circulation anomaly can be maintained until summer.

In summer, the zonal circulation induced by the SSTG produces anomalous lower-level vorticity and vertical wind shear (VWS) patterns over the WNP and a mid-tropospheric westerly anomaly over Chinese coastal regions, which are unfavorable for TCs making landfall in mainland China. Here, the VWS is defined as follows:

$$\mathrm{VWS} = [(u_{850} - u_{200})^2 + (v_{850} - v_{200})^2]^{\frac{1}{2}} ,$$

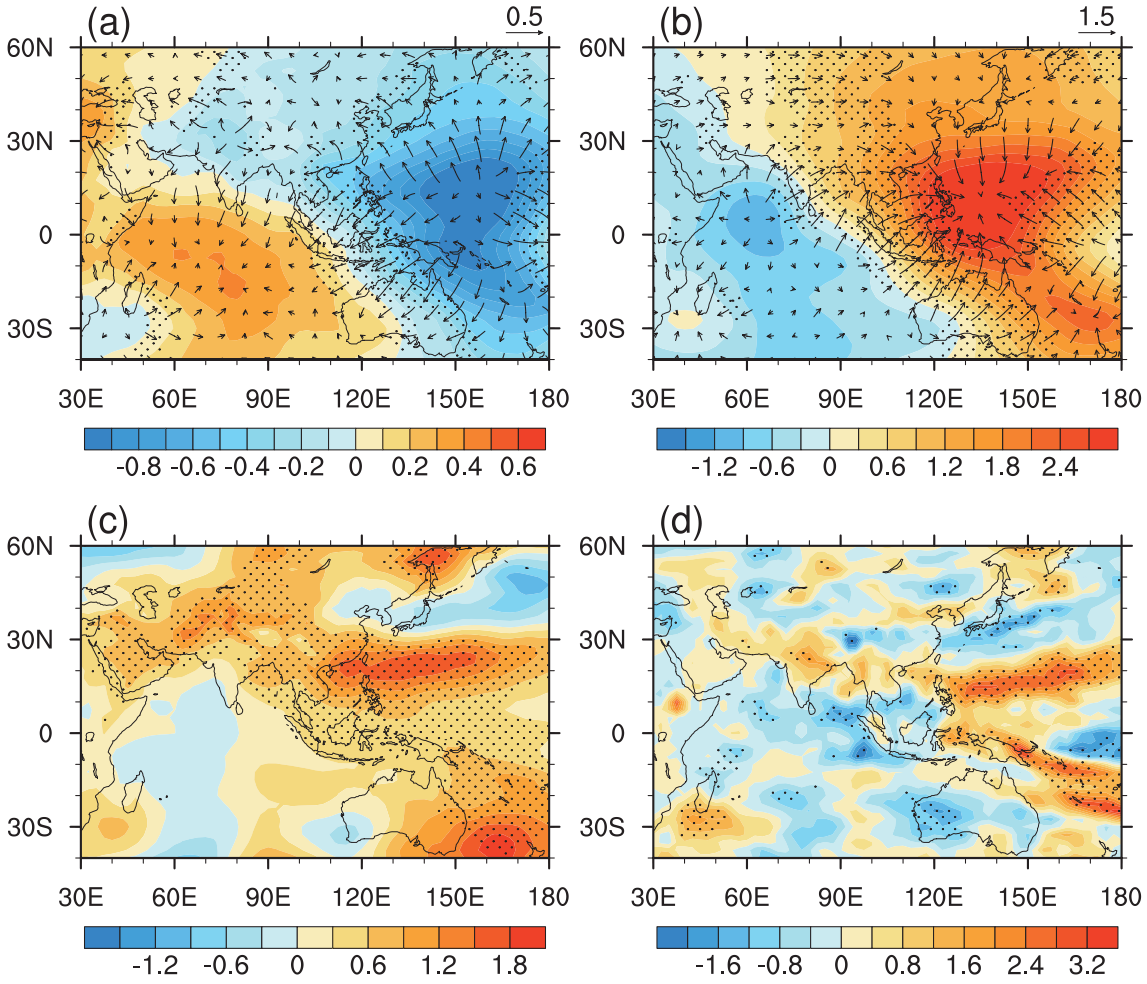

Fig. 4. Regression patterns of seasonal mean (a) 850-hPa and (b) 200-hPa divergent winds (vectors) and velocity potential ($\times 10^6$; color-shaded), (c) SLP ($\times 10^2$), and (d) 500-hPa vertical pressure velocity ($\times 10^{-2}$) in summer with respect to the spring SSTG during 1979–2015. Stippling denotes regions where the differences in the zonal divergent winds at 850 hPa in (a), zonal divergent winds at 200 hPa in (b), SLP in (c), and vertical pressure velocity at 500 hPa in (d), are significant at the 90% confidence level, according to the Student's *t*-test.

where u_{850} and u_{200} represent the 850 hPa and 200 hPa zonal wind components, respectively. v_{850} and v_{200} denote the 850 hPa and 200 hPa meridional wind components, respectively.

As shown in Fig. 5a, a positive SSTG generates an apparent tripole pattern of lower-level vorticity anomalies over the WNP. That is, positive lower-level vorticity anomalies appear from the Yellow Sea to the east of Japan; negative anomalies from the South China Sea to the east of Taiwan; and positive anomalies over regions close to the equator. These lower-level vorticity anomalies are accompanied by positive VWS anomalies over the east of East Asia and negative anomalies around the Philippines (Fig. 5b). It can be seen that these two key environmental fields favorable for TC genesis concentrate around the Philippines. Moreover, an evident lower-level anomalous anticyclone basically occupies the main TC genesis area (5°–35°N, 100°–170°E), where TC genesis frequency accounts for about 94% of the total over the WNP in summer during the period 1979–2015 (Fig. 5c). In the same period, the correlation between the spring SSTG and the summer TC genesis frequency over this area is about −0.43, exceeding the 99% confidence level.

The LTC activity is closely associated with TC genesis location and steering flow (e.g., Goh and Chan, 2010; Mei et al., 2015). As shown in Fig. 5c, corresponding to the above-mentioned main WNP TC genesis region, there is a mid-tropospheric positive geopotential anomaly. This primarily modulates the large-scale mid-tropospheric flows, which can markedly affect TC movement (Chan and Gray, 1982). As demonstrated in Fig. 5d, anomalous westerlies (easterlies) dominate over (20°–40°N, 100°–130°E) (the Philippines and southern Vietnam) in the middle troposphere. This anomalous circulation pattern suppresses TC occurrence to the east of Southeast China and, moreover, is unfavorable for steering TCs westward to make landfall in mainland China.

In addition, we investigate the lag correlations between the spring SSTG and the key variable fields mentioned above in the following months, so as to identify how the influence of the preconditioned environmental fields on LTCs in main-

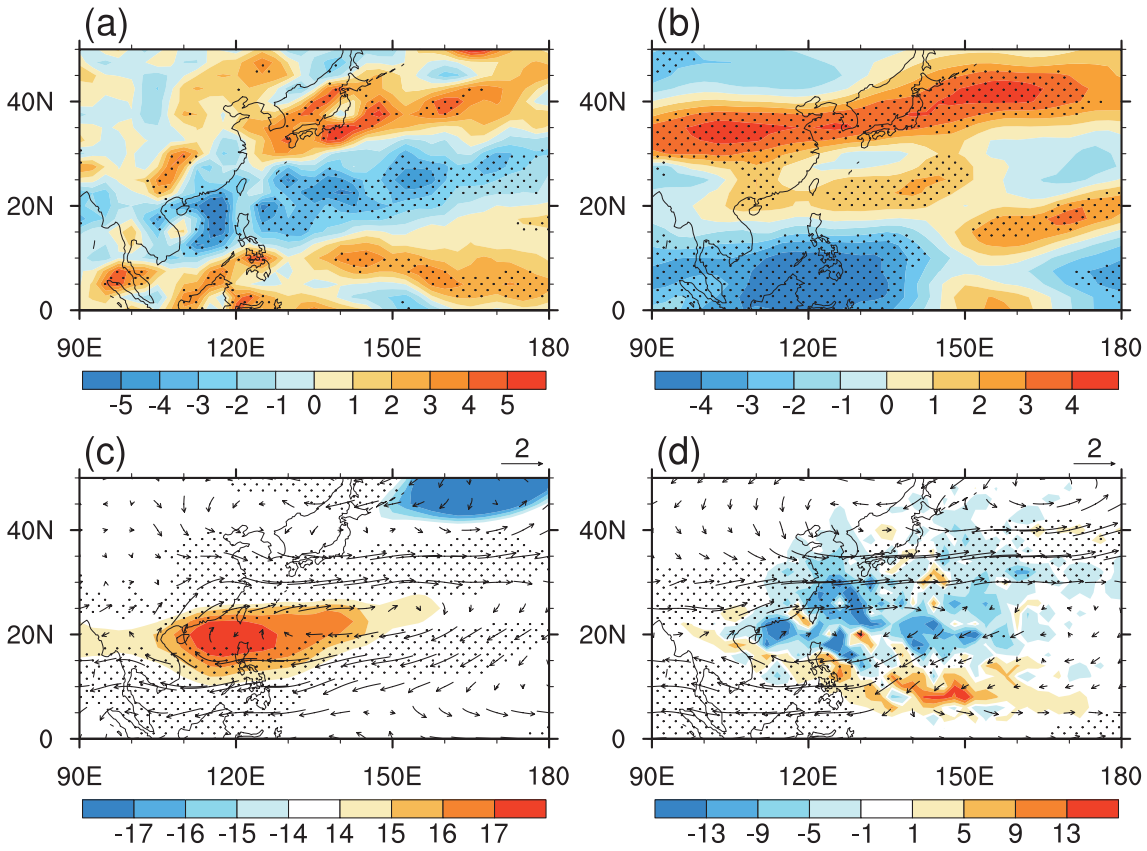

Fig. 5. Regression patterns of seasonal mean (a) 850-hPa relative vorticity ($\times 10^{-6}$), (b) vertical wind shear between 850 and 200 hPa, (c) 850-hPa winds (vectors) and 500-hPa geopotential ($\times 10^{1}$; color-shaded), and (d) 500-hPa winds (vectors) and TC frequency ($\times 10^{-1}$; color-shaded) measured by the total TC occurrence in every $2^\circ \times 2^\circ$ box in summer with respect to the spring SSTG during 1979–2015. Stippling denotes regions where the differences in the relative vorticity at 850 hPa in (a), vertical wind shear between 850 and 200 hPa in (b), zonal winds at 850 hPa in (c), and zonal winds at 500 hPa in (d), are significant at the 90% confidence level, according to the Student's *t*-test.

land China is maintained. By producing anomalous environmental fields over the WNP, the zonal circulation anomaly can significantly impact LTCs in mainland China throughout summer. Thus, several dynamic variables are selected based on the regressed patterns in Figs. 4 and 5, including the lower-level divergent zonal winds averaged over (10°S–15°N, 95°–125°E), the upper-level divergent zonal winds averaged over (5°–20°N, 65°–125°E), the SLP gradient measured as the difference between the SLP averaged over (20°S–10°N, 55°–75°E) and that averaged over (10°–20°N, 110°–150°E), the mid-tropospheric vertical pressure velocity (MVPV) difference between the MVPV averaged over (15°S–10°N, 40°–90°E) and that averaged over (0°–20°N, 125°–155°E), the lower-level relative vorticity averaged over (15°–30°N, 110°–180°E), and the mid-tropospheric zonal winds averaged over (20°–40°N, 110°–130°E).

From March to September, the negative correlations between the spring SSTG and the lower-level zonal divergent winds and the SLP gradient are significant in spring and summer (Figs. 6a and c). Figure 6b shows that the significant positive correlation between the spring SSTG and the upper-level zonal divergent winds can persist from March to August. Throughout spring and summer, significant correlation above the 95% confidence level exists between the spring SSTG and the mid-tropospheric vertical pressure velocity difference (Fig. 6d). Besides, the negative correlation between the spring SSTG and the lower-level relative vorticity is also significant in summer (Fig. 6e), especially in July. Throughout summer, significant correlation above the 95% confidence level exists between the spring SSTG and the mid-tropospheric zonal winds (Fig. 6f). These correlations show a pathway for the spring SSTG impacting TC landfall in mainland China throughout the following summer.

5. Summary

The summer LTC frequency in mainland China is significantly related to the spring SSTG between the TIO and the WWP. The connection between them may be explained by the atmospheric response in summer to the SSTG in spring and the air–sea interaction in summer triggered by the spring SSTG anomaly. In spring, a positive SSTG results in a zonal pressure gradient, which induces an anomalous zonal inter-basin circulation. Lower-level convergence, ascent, and upper-level divergence develop over the TIO, while upper-

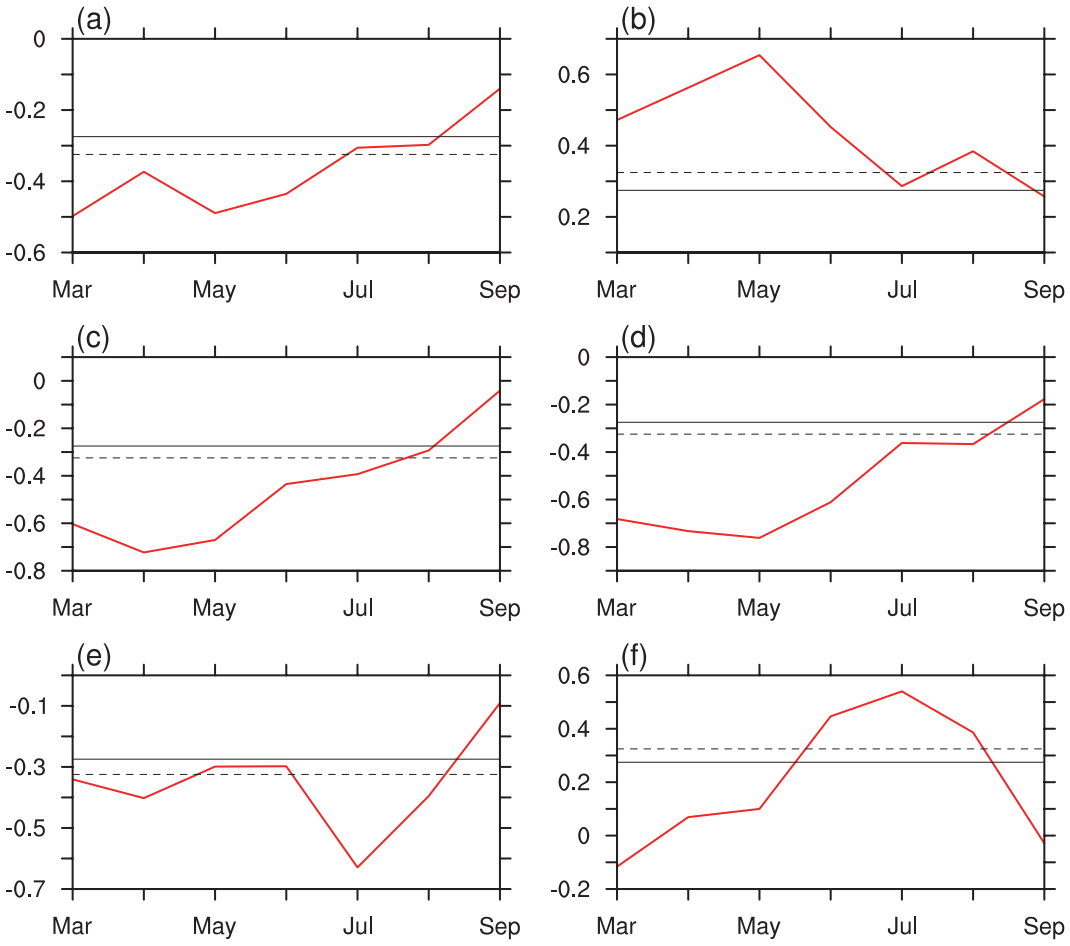

Fig. 6. Lag correlations between the SST gradient in spring and monthly mean (a) 850-hPa zonal divergent winds (10°S–15°N, 95°–125°E), (b) 200-hPa zonal divergent winds (5°–20°N, 65°–125°E), (c) the SLP gradient between (20°S–10°N, 55°–75°E) and (10°–20°N, 110°–150°E), (d) the 500-hPa vertical p-velocity difference between (15°S–10°N, 40°–90°E) and (0°–20°N, 125°–155°E), (e) 850-hPa relative vorticity (15°–30°N, 110°–180°E), and (f) 500-hPa zonal winds (20°–40°N, 110°–130°E), from March to September during 1979–2015. The solid (dashed) transverse line indicates correlations significant at the 90% (95%) confidence level.

level convergence, descent, and lower-level divergence develop over the WWP, producing lower-level anomalous easterlies and upper-level anomalous westerlies between the TIO and WWP. After being triggered, the anomalous inter-basin circulation facilitates a warming of the west-central TIO by prohibiting local oceanic upwelling and driving warm water westward from the east and a cooling of the WWP by inducing local upwelling, which maintains the anomalous inter-basin circulation until summer. Consequently, the anomalous inter-basin circulation induces anomalous lower-level negative vorticity and strong vertical wind shear over most of the regions to the north of Luzon Island, and a lower-level anticyclone over the main WNP TC genesis region (5°–35°N, 100°–170°E), which is unfavorable for TC genesis. Corresponding to this main TC genesis region, there is an anomalous mid-tropospheric anticyclone, meaning westerlies (easterlies) appear over the coastal regions of mainland China (the Philippines and the southern Vietnam), which are unfavorable for steering TCs to make landfall in mainland China in summer. In contrast, a negative spring SSTG produces environmental fields favorable for TCs making landfall in mainland China in summer.

Acknowledgements. The authors are grateful to the anonymous reviewers for their helpful comments. This study was supported by the National Natural Science Foundation of China (Grant Nos. 41461164005, 41375065 and 41475074).

REFERENCES

Chan, J. C. L., and W. M. Gray, 1982: Tropical cyclone movement and surrounding flow relationships. *Mon. Wea. Rev.*, **110**, 1354–1374.

Dee, D. P., and Coauthors, 2011: The ERA-Interim reanalysis: configuration and performance of the data assimilation system. *Quart. J. Roy. Meteor. Soc.*, **137**, 553–597, http://dx.doi.org/10.1002/qj.828.

Du, Y., L. Yang, and S.-P. Xie, 2011: Tropical Indian Ocean influence on northwest Pacific tropical cyclones in summer following strong El Niño. *J. Climate*, **24**, 315–322, http://doi.org/

10.1175/2010JCLI3890.1.

Emanuel, K., 2003: Tropical cyclones. *Annual Review of Earth and Planetary Sciences*, **31**, 75–104, http://doi.org/10.1146/annurev.earth.31.100901.141259.

Goh, A. Z. C., and J. C. L. Chan, 2010: An improved statistical scheme for the prediction of tropical cyclones making landfall in South China. *Wea. Forecasting*, **25**, 587–593, http://doi.org/10.1175/2009WAF2222305.1.

Gray, W. M., 1979: Hurricanes: Their formation, structure and likely role in the tropical circulation. *Meteorology over the Tropical Oceans*, D. B. Shaw, Ed., Royal Meteorological Society, 155–218.

Ho, C. H., J. J. Baik, J. H. Kim, D. Y. Gong, and C. H. Sui, 2004: Interdecadal changes in summertime typhoon tracks. *J. Climate*, **17**, 1767–1776, https://doi.org/10.1175/1520-0442(2004)017<1767:ICISTT>2.0.CO;2.

Knapp, K. R., M. C. Kruk, D. H. Levinson, H. J. Diamond, and C. J. Neumann, 2010: The International Best Track Archive for Climate Stewardship (IBTrACS): Unifying tropical cyclone data. *Bull. Amer. Meteoro. Soc*., **91**, 363–376, http://doi.org/10.1175/2009BAMS2755.1.

Kossin, J. P., and D. J. Vimont, 2007: A more general framework for understanding Atlantic hurricane variability and trends. *Bull. Amer. Meteor. Soc*., **88**, 1767–1781, http://doi.org/10.1175/BAMS-88-11-1767.

Li, R. C. Y., and W. Zhou, 2012: Changes in western Pacific tropical cyclones associated with the El Niño-Southern Oscillation cycle. *J. Climate*, **25**, 5864–5878, http://doi.org/10.1175/JCLI-D-11-00430.1.

Li, R. C. Y., and W. Zhou, 2014: Interdecadal change in South China Sea tropical cyclone frequency in association with zonal sea surface temperature gradient. *J. Climate*, **27**, 5468–5480, http://doi.org/10.1175/JCLI-D-13-00744.1.

Liu, K. S., and J. C. L. Chan, 2003: Climatological characteristics and seasonal forecasting of tropical cyclones making landfall along the South China coast. *Mon. Wea. Rev*., **131**, 1650–1662, http://doi.org/10.1175//2554.1.

Mei, W., S.-P. Xie, M. Zhao, and Y. Q. Wang, 2015: Forced and internal variability of tropical cyclone track density in the western North Pacific. *J. Climate*, **28**, 143–167, http://doi.org/10.1175/JCLI-D-14-00164.1.

Rayner, N. A., D. E. Parker, E. B. Horton, C. K. Folland, L. V. Alexander, D. P. Rowell, E. C. Kent, and A. Kaplan, 2003: Global analyses of sea surface temperature, sea ice, and night marine air temperature since the late nineteenth century. *J. Geophys. Res*., **108**(D14), 4407, http://doi.org/10.1029/2002JD002670.

Tao, L., L. G. Wu, Y. Q. Wang, and J. L. Yang, 2012: Influence of tropical Indian Ocean warming and ENSO on tropical cyclone activity over the western North Pacific. *J. Meteor. Soc. Japan*, **90**, 127–144, http://doi.org/10.2151/jmsj.2012-107.

Vimont, D. J., and J. P. Kossin, 2007: The Atlantic meridional mode and hurricane activity. *Geophys. Res. Lett*., **34**, L07709, http://doi.org/10.1029/2007GL029683.

Wang, L., and R. G. Wu, 2012: In-phase transition from the winter monsoon to the summer monsoon over East Asia: Role of the Indian Ocean. *J. Geophys. Res*., **117**, D11112, http://doi.org/10.1029/2012JD017509.

Wu, M. C., W. L. Chang, and W. M. Leung, 2004: Impacts of El Niño–Southern Oscillation events on tropical cyclone landfalling activity in the western North Pacific. *J. Climate*, **17**, 1419–1428, https://doi.org/10.1175/1520-0442(2004)017<1419:IOENOE>2.0.CO;2.

Xie, S.-P., K. M. Hu, J. Hafner, H. Tokinaga, Y. Du, G. Huang, and T. Sampe, 2009: Indian Ocean capacitor effect on Indo-western Pacific climate during the summer following El Niño. *J. Climate*, **22**, 730–747, https://doi.org/10.1175/2008JCLI2544.1.

Xie, S.-P., Y. Kosaka, Y. Du, K. M. Hu, J. S. Chowdary, and G. Huang, 2016: Indo-western Pacific Ocean capacitor and coherent climate anomalies in post-ENSO summer: A review. *Adv. Atmos. Sci.*, **33**, 411–432, http://doi.org/10.1007/s00376-015-5192-6.

Yang, J. L., Q. Y. Liu, S.-P. Xie, Z. Y. Liu, and L. X. Wu, 2007: Impact of the Indian Ocean SST basin mode on the Asian summer monsoon. *Geophys. Res Lett*., **34**, L02708, http://doi.org/10.1029/2006GL028571.

Zhan, R. F., Y. Q. Wang, and X. T. Lei, 2011a: Contributions of ENSO and east Indian Ocean SSTA to the interannual variability of northwest Pacific tropical cyclone frequency. *J. Climate*, **24**, 509–521, https://doi.org/10.1175/2010JCLI3808.1.

Zhan, R. F., Y. Q. Wang, and C.-C. Wu, 2011b: Impact of SSTA in the east Indian Ocean on the frequency of northwest Pacific tropical cyclones: A regional atmospheric model study. *J. Climate*, **24**, 6227–6242, https://doi.org/10.1175/JCLI-D-10-05014.1.

Zhan, R. F., Y. Q. Wang, and M. Ying, 2012: Seasonal forecasts of tropical cyclone activity over the western North Pacific: A review. *Tropical Cyclone Research and Review*, **1**, 307–324, https://doi.org/10.6057/2012TCRR03.07.

Zhan, R. F., Y. Q. Wang, and M. Wen, 2013: The SST gradient between the southwestern Pacific and the western Pacific warm pool: A new factor controlling the northwestern Pacific tropical cyclone genesis frequency. *J. Climate*, **26**, 2408–2415, https://doi.org/10.1175/JCLI-D-12-00798.1.

Zhao, J. W., R. F. Zhan, Y. Q. Wang, and L. Tao, 2016: Intensified interannual relationship between tropical cyclone genesis frequency over the Northwest Pacific and the SST gradient between the Southwest Pacific and the western Pacific warm pool since the mid-1970s. *J. Climate*, **29**, 3811–3830, https://doi.org/10.1175/JCLI-D-15-0729.1.